ELSEVIER

Colloids and Surfaces
A: Physicochemical and Engineering Aspects 96 (1995) 171–179

COLLOIDS AND SURFACES A

Amphiphiles at oil–water interfaces: simulation study of their tension-reducing properties

K.J. Klopfer, T.K. Vanderlick *

University of Pennsylvania, Department of Chemical Engineering, 220 South 33rd Street, Philadelphia, PA 19104-6393, USA

Received 22 July 1994; 31 October 1994

Abstract

Molecular dynamics simulations of amphiphiles at a mock oil–water interface have been carried out using a simple well-known model which represents amphiphiles as conglomerates of water and oil particles connected together with harmonic potentials. We studied the tension reduction properties of amphiphiles composed of one water and one or more oil particles connected in a series; we varied the length of the series and placement of the water particle within it. In comparing amphiphiles of fixed length, we find that those with a terminal water particle are most effective at reducing the tension; these molecules mimic single-chained (the others, double-chained) amphiphiles. We find that at low concentrations, all amphiphiles examined behaved as insoluble monolayers. In this regime, we attempted to apply two-dimensional equations of state to predict their tension-reduction properties. At higher concentrations, the amphiphiles exhibit an increased solubility in the bulk oil phase, but are believed not to be in their most stable state.

Keywords: Amphiphile; Interfacial tension; Molecular dynamics simulation

1. Introduction

The interface that forms between oil and water is a natural habitat for amphiphiles. These molecules, which have both hydrophobic and hydrophilic parts, can cope with their dual character by residing at the oil–water interface, and in doing so act to lower the tension between the two immiscible fluids. The tension-reducing effect of amphiphiles is related to their concentration, and also to the molecular make-up of the amphiphiles themselves.

The phase behavior of amphiphile–oil–water mixtures is both rich and spectacular. A plethora of fluid microstructures — amongst these micelles and microemulsions — can be formed as the relative concentrations of water to oil to amphiphile are varied. A planar interface hosting amphiphiles is merely one of the simplest possibilities.

The properties of oil–water–amphiphile systems are exploited in a variety of industries, two of the most prominent being petroleum recovery and food processing. In spite of their vast presence and importance, oil–water–amphiphile systems have not been the focus of much computer-simulation-based research. In contrast, extensive simulations have been carried out to investigate the behavior of amphiphiles on solids [1–3], and amphiphiles at the liquid–vapor interface [4–6]. One key driving force behind this emphasis has been the projected technological promise of Langmuir–Blodgett films [7]: these are formed by transferring

* Corresponding author.

SSDI 0927-7757(94)03056-1

insoluble monolayers from the water surface onto a solid support as the substrate is passed through the air–water interface.

Despite the advances in computational power, current computer simulations of amphiphiles at interfaces cannot account for all essential degrees of freedom. Detailed modelling of the amphiphiles is often accomplished at the expense of a molecular description of one, or both, bulk phases; their presence is then often treated by way of external potentials [5,6]. This approach is useful when solid or vapor phases are present, another factor contributing to the preponderance of these simulations. This approach is not as suitable for oil–water–amphiphile simulations, since the molecular nature of all components plays a significant role in establishing the structure and properties of these systems.

An alternative strategy is to relinquish a detailed molecular model of the amphiphiles in exchange for a particulate representation of all components. Amphiphiles are then modeled as conglomerates of two different particle types, one representing oil in the simulation and the other water. This approach was taken by Larson et al. [8–10] over 15 years ago in their Monte Carlo lattice simulations of oil–water–amphiphile systems. They saw the self-assembly of lamellar arrays, cylinders, and spheres. More recently, Mareschal and co-workers [11,12] used this approach to study the kinetics of adsorption of amphiphiles at fluid–fluid interfaces. Smit and co-workers [13–16] have also exploited this methodology to study the tension-reducing properties of some linear and branched chain amphiphiles.

One key finding supported by all the simulations just mentioned is that this simple description of amphiphiles is able to capture, at least qualitatively, much of the underlying physics of amphiphilic behavior. One of the triumphs in this regard has been the demonstration of micelle formation as seen in the large-scale simulation (based on 39 000 particles) recently conducted by Smit et al. [16]. Hence simulations of this general nature serve as useful tools for probing the fundamental behavior of amphiphile–water–oil systems; under present computational limitations, they may be one of the few tools available for investigating some of the more complex phenomena of interest, such as the structure and phase behavior of systems containing more than one type of amphiphile.

As a stepping stone towards more complicated applications, it is worthwhile to examine more closely and fully predictions of such simulations for simple systems. For example, Smit and co-workers [13–15] observe a nearly linear decrease in the tension of a planar oil–water interface as the overall concentration of amphiphiles in the system is increased. The slope of this decrease depends on the architecture of the amphiphile; for instance it is larger for amphiphiles with longer hydrophobic chains. In this paper, we pursue further the effect of architecture on the tension-reduction properties, and interpret the concentration dependence of tension in terms of two-dimensional equations of states for insoluble monolayers.

2. Model and computational details

The model used was inspired by the free energy density functional theory developed by Telo da Gama and Gubbins [17]. Each particle in the simulation can be identified as one of two species: oil or water. Amphiphiles are nothing more than water and oil particles connected via Hookean springs; this construction captures, at a basic level, the dual hydrophilic/hydrophobic character of these molecules. By connecting different amounts of particles in different configurations, this simple approach can be used to create molecules with varying architectures.

The two species of particles interact with truncated Lennard-Jones potentials with energy parameter ϵ_{ij}, distance parameter σ_{ij} and cut-off radius R_{ij}^{cut}

$$\phi_{ij} = \begin{cases} \phi_{ij}(r) - \phi_{ij}(R_{ij}^{\text{cut}}) & r \leqslant R_{ij}^{\text{cut}} \\ 0 & r \leqslant R_{ij}^{\text{cut}} \end{cases}$$

$$\phi_{ij} = 4\epsilon_{ij}\left[\left(\frac{\sigma_{ij}}{r}\right)^{12} - \left(\frac{\sigma_{ij}}{r}\right)^{6}\right]$$

We have assumed that all interactions are governed by the same σ and ϵ. Therefore, the only difference

between oil–oil, water–water, and oil–water interactions is spelled out in the choice of R_{ij}^{cut}. Intraspecies interactions have $R_{ij}^{cut}=2.5\sigma$, and thus include both the attractive and repulsive portions of the Lennard-Jones potential. On the other hand, the interspecies interactions have $R_{ij}^{cut}=2^{1/6}\sigma$, restricting the interactions to being repulsive. The lack of attractive forces between oil and water particles induces their separation into two phases. We note here that the potential above is just one that can be used to model amphiphiles at fluid–fluid interfaces: instead of using a strict cut-off to differentiate interspecies and intraspecies interactions, Mareschal and co-workers [11,12] employed a two-parameter variation of the Lennard-Jones potential in their simulations.

From the total number of particles in a simulation, a requisite fraction of water and oil particles is used to create amphiphiles (in keeping track of density profiles, these are no longer identified as water or oil particles, but rather as segments of amphiphiles). Amphiphiles are constructed by adding to the potential above (which continues to apply to all particles) harmonic potentials between designated pairs of their constituent particles. For this we use

$$\phi_{ij}=\frac{1}{2}k(r_{ij}-\sigma)^2$$

where k is the spring constant, and σ is the separation at zero force. The value of k employed in the simulations should not affect the tension calculation and we show evidence of this in the appendix.

In our simulations we have used a system of 1300 particles in a rectangular box of size $8.939\sigma \times 8.939\sigma \times 23.24\sigma$. Periodic boundary conditions are kept in all three directions and the length in the z-direction is large enough such that molecules at opposite interfaces cannot interact with one another. The overall density was $\rho=0.7\sigma^{3}$ and a constant temperature of $T=1\epsilon/k_b$ (where k_b is Boltzmann's constant) was maintained by incorporating a constraint method into our leap-frog verlet algorithm as described by Allen and Tildesley [18].

We have found that when the oil and water start out well-mixed, approximately 4×10^4 time steps are needed before phase separation occurs. In order to save this extra equilibration time, the system is started out in a phase separated pattern with one layer of water particles (325 total) sandwiched between two layers of oil particles (975 total). From this set of particles, amphiphiles are defined by choosing a water particle from those lying within 3σ of an oil layer and then choosing the requisite number of oil particles. The latter are selected at random under the condition that no connected segments are separated by more than 10σ. So as to ease the connected segments in closer, the spring constant is started from an initial value of $1.0\epsilon/\sigma^{-2}$ and slowly ramped to its final value of $1 \times 10^5\epsilon/\sigma^{-2}$ over 5×10^3 time steps. We use a time step of 0.005τ, where $\tau=\sigma(m/\epsilon)^{1/2}$; here m is the particle mass.

Starting up from the configuration just described, we find that thermodynamic quantities have stabilized by about 2×10^4 time steps; we allow, however, an additional 2×10^4 steps to pass before equilibrium is assumed. Data are then collected for 1.2×10^5 time steps. At every time step, the interfacial tension was calculated from the atomic virial [4]. The accuracy of our simulations was estimated by dividing the data collection steps into subruns of 1×10^4 time steps, determining the average interfacial tension within each subrun, and calculating its standard deviation from subrun averages (this is the error in tension which we report). Density profiles, and also components of the pressure tensor [16], were calculated only during one subrun (usually the next to last), at every time step within it. Density profiles shown herein represent the subrun averaged profile. Pressure profiles, which are not shown, were calculated to assure the constancy of normal pressure throughout the simulation box.

3. Results and discussion

The amphiphiles examined in this study are all composed of one water particle and one or more oil particles; the particles are connected to one another in series to form a train. Two features account for differences between the amphiphiles: (1) the number of oil particles included in the train;

(2) the placement of the water particle in the train. The first feature establishes the size of the amphiphile and its ratio of hydrophobic to hydrophilic moieties. Trains of two different lengths were examined: one containing four oil particles (henceforth denoted (4:1)), the other containing six (henceforth denoted (6:1)). The second feature serves to probe the influence of molecular architecture. Trains having a terminal water particle mimic linear single-chained amphiphiles. Trains containing a non-terminal water particle mimic double-chained amphiphiles; the relative lengths of the two chains are controlled by the position of the water particle — or "headgroup" — within the train. Table 1 lists the different amphiphiles examined in this study, their number in each simulation, and the corresponding interfacial tension as established in each simulation.

Fig. 1 shows the variation of tension with number of amphiphiles, plotted for two different architectures having the same hydrophobic to hydrophilic ratio (4:1) — a single-chained configuration and a symmetric double-chained configuration. As is readily seen, the observed tension is sensitive to the architecture of the amphiphile, with differences becoming more pronounced (and statistically significant) as the concentration increases. In general, the single-chained configuration is more effective than the double-chained configuration at reducing the interfacial tension.

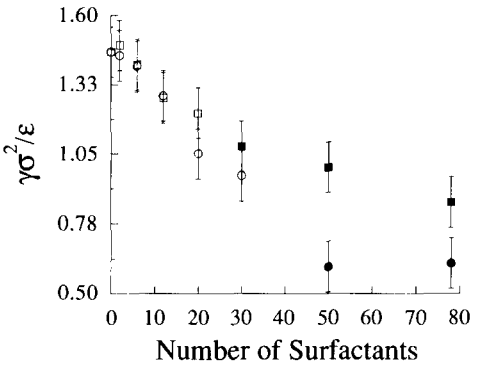

Fig. 1. The dimensionless interfacial tension ($\gamma\sigma^2/\epsilon$) vs. number of surfactants for (□) double chain, dilute regime; (○) single chain, dilute regime; (■) double chain, concentrated regime; (●) single chain, concentrated regime.

Although we did not carry out as many simulations for the (6:1) amphiphile, we expect the same architecture dependence to exist (tensions reported in Table 1 for the (6:1) amphiphiles are not at high enough concentrations to show significant differences).

Fig. 1 also reveals a general trend, followed for each specific amphiphile examined: the concentration dependence of tension can be broken into two nearly linear regimes. We henceforth refer to the one spanning lower concentrations as the dilute regime, and the other as the concentrated regime. To facilitate the observation of these regimes in

Table 1
The dimensionless interfacial tension ($\gamma\sigma^2/\epsilon$) as a function of total number of amphiphiles for a variety of architectures

Interfacial tensions (4:1) amphiphiles			Number	Interfacial tensions (6:1) amphiphiles		
						
–	1.48 ± 0.08	1.44 ± 0.08	2			–
–	1.41 ± 0.09	1.40 ± 0.09	6	1.40 ± 0.09	1.37 ± 0.10	1.36 ± 0.10
1.33 ± 0.09	1.28 ± 0.10	1.27 ± 0.10	12	–		–
–	1.21 ± 0.10	1.23 ± 0.11	20	1.01 ± 0.11	1.13 ± 0.10	1.13 ± 0.12
1.06 ± 0.11	1.08 ± 0.11	0.96 ± 0.09	30	–	–	–
0.93 ± 0.11	1.00 ± 0.10	0.61 ± 0.11	50			–
–	0.86 ± 0.11	0.62 ± 0.11	78	–	–	–

Fig. 1, the simulation results in the dilute regime are distinguished with empty symbols; those in the concentrated regime with filled symbols. We note here that Smit and co-workers also report a linear decrease in tension in their simulations of single-chained [14,15] and branched-chained [13] amphiphiles, but a cross-over to a second linear regime was not observed.

Examination of the density profiles establishes the underlying difference between the dilute and concentrated regimes. Fig. 2 shows density profiles of the head group of the single-chained amphiphile (4:1) at four different concentrations. As is readily seen, in the dilute regime (see Fig. 2A) amphiphiles are present solely at the interface between the oil and water phases; in the concentrated regime (see Fig. 2B), amphiphiles are also present in the oil phase.

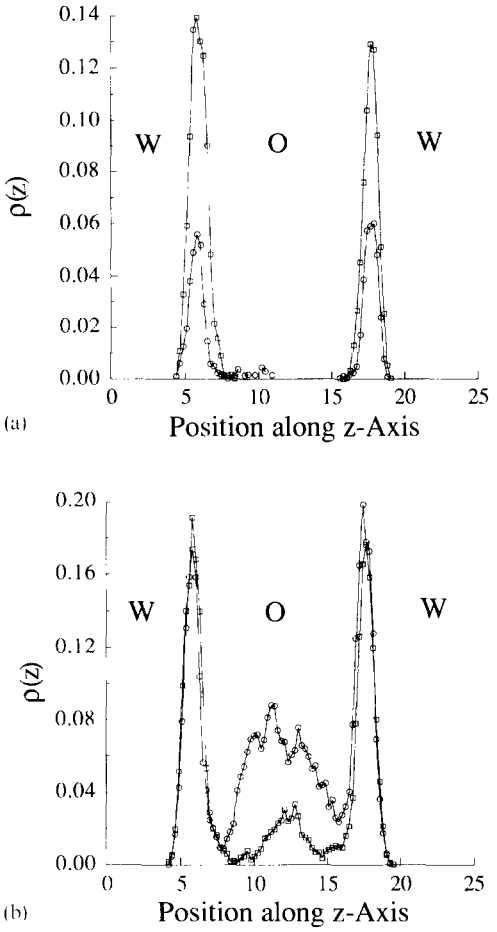

Fig. 2. The density profile of head group vs. position along the z-axis (σ) for (a) 12 amphiphiles (○), 30 amphiphiles (□), (b) 50 amphiphiles (◧), 78 amphiphiles (●) (where W denotes the location of the water bulk phases and O denotes the location of the oil bulk phase).

For all amphiphiles that were examined, the density profiles exhibited the same general characteristics. In the dilute regime, as the concentration of amphiphiles is increased the head group density profile becomes higher but not significantly broader; the interface stays sharp as it becomes loaded with the amphiphiles. Throughout the concentrated regime, the interface stays sharp and hosts roughly the same amount of amphiphiles; the excess amphiphiles are accepted by the oil phase. The transition from the dilute to concentrated regime thus occurs when the interface can no longer easily accommodate more amphiphiles. In what follows we analyze in more detail each of these two regimes.

One of the most interesting features observed in the concentrated regime is the appearance of a depletion region separating amphiphiles at the interface from amphiphiles residing in the bulk oil phase. Although no specific mention of this was made, Smit et al. [16] see a similar region in their simulation of single-chained amphiphiles; a depletion region on the oil side of the interface can be seen in their reported snapshots. In their simulations, which were based on much larger numbers of particles than ours, Smit et al. [16] also observe the formation of micelles in the water phase, and they make particular note of a similar depletion region occurring on the water side of the interface.

Since amphiphiles are distributed throughout the oil phase, we attempted to apply the Gibbs adsorption equation [19] (assuming ideal solution behavior) to predict the decrease in tension as a function of their concentration

$$d\gamma/kT = -\Gamma d \ln c$$

where γ is the interfacial tension, c is the concentration of amphiphiles in the bulk, and Γ is the surface excess of amphiphiles (which we base on a dividing surface yielding no surface excess of oil particles). The local densities in the middle of the oil phase were used to estimate the bulk concentrations of oil and amphiphiles; from these the

dividing surface and Γ were determined. In doing so, we found that the predicted decrease in tension was much larger than that measured in the simulations. The failure of the Gibbs adsorption equation (with due caveat to the applicability of the ideal solution estimation of chemical potential) is one signature that the system is not in a state of thermodynamic equilibrium. This is not surprising in light of the micelle formation observed in the large-scale simulation of Smit et al. [16]; the overall concentration of amphiphiles examined in their simulation falls within the range corresponding to the concentrated regime reported herein. Apparently, the smaller size of our simulation precludes the formation of certain microstructures, such as micelles. It is possible that, in our simulations, the cross-over from the dilute to concentrated regimes represents the CMC.

In the dilute regime, the amphiphiles are located solely at the interface, and so two-dimensional equations of state derived for insoluble monolayers provide a framework for analyzing and interpreting those simulation results. Such equations of state are given in terms of the surface pressure, defined as $\pi = \gamma_0 - \gamma$, where γ_0 is the tension of the bare oil–water interface. In a separate simulation, we determined the latter to be $1.45 \pm 0.10(\gamma\sigma^2/\epsilon)$.

The simplest equation of state is, of course, an ideal gas formulation $\pi A = NkT$, where A is the interfacial area (established by the size of the simulation box) and N is the number of amphiphiles in the system. This equation predicts a linear decrease in tension with N, but one that is independent of any molecular detail associated with the amphiphiles. Since architecture and chain length do indeed influence the tension-reducing properties of amphiphiles, the ideal gas equation of state is clearly not viable.

A simple equation of state that incorporates molecular size effects, and thus offers a route to account for the observed dependence of tension on molecular architecture, can be written

$$\pi(A - NA_0) = NkT \tag{1}$$

where A_0 represents the excluded area per molecule. A measure of the interfacial area taken up by the amphiphiles can be determined in the simulations. For each amphiphile, we projected the positions of its constituent particles onto the x–y plane (which is parallel to the interface), and found the diameter of the smallest disk, D, which encompasses all the points. An estimate of A_0 is then given by $\pi(D + \sigma)^2/4$, where σ is added to D to take into account the radii of the particles. The average disk diameters determined in the simulations are reported in Table 2.

Some interesting observations are evident on examining Table 2. The first is that, for a given architecture, the disk diameter stays fairly constant regardless of the number of amphiphiles residing

Table 2
The disk diameter (σ) as a function of total number of amphiphiles for a variety of architectures

Disk diameter (4:1) amphiphiles			Number	Disk diameter (6:1) amphiphiles		
						
–	2.06 ± 0.36	1.81 ± 0.35	2	–	–	–
–	2.11 ± 0.20	1.91 ± 0.19	6	2.51 ± 0.24	2.65 ± 0.22	2.66 ± 0.26
–	2.03 ± 0.13	1.75 ± 0.12	12	–	–	–
–	2.03 ± 0.10	1.87 ± 0.11	20	2.36 ± 0.13	2.70 ± 0.12	2.49 ± 0.15
–	2.01 ± 0.09	1.80 ± 0.09	30	–	–	–
1.96 ± 0.08	2.03 ± 0.05	1.80 ± 0.06	50	–	–	–
–	2.01 ± 0.06	1.90 ± 0.06	78	–	–	–

at the interface. This holds even for the most dilute systems, implying that lone amphiphiles are not lying flat on the interface. Other observations are less surprising. In general, the disk diameters for double-chained amphiphiles are larger than those for single-chained amphiphiles having the same hydrophobic/hydrophilic content. Since the water particle serves to pin the amphiphile to the interface, amphiphiles constructed with non-terminal water particles cannot extend away from the interface as sharply as those constructed with terminal water particles. For this same reason, unsymmetrical double-chained configurations exhibit disk diameters (and also interfacial tensions) that are closer to those of symmetrical double-chained, as opposed to single-chained, configurations. Finally, for a given architecture, longer amphiphiles exhibit larger disk diameters, as might be expected.

The simulation results for D, and thereby A_0 (according to the prescription above) were used to examine the performance of Eq. 1. Fig. 3 shows tensions obtained in simulations along with equation of state predictions for two different amphiphiles — the single-chained and the symmetric double-chained (4:1). For each amphiphile, A_0 was determined using an average value of D, computed from those values falling in the dilute regime ($N=2$, 6, 12, 20). As can be seen, the equation of state does a good job at predicting the tension over a significant fraction of the dilute regime, with departures occurring only at the higher concentrations.

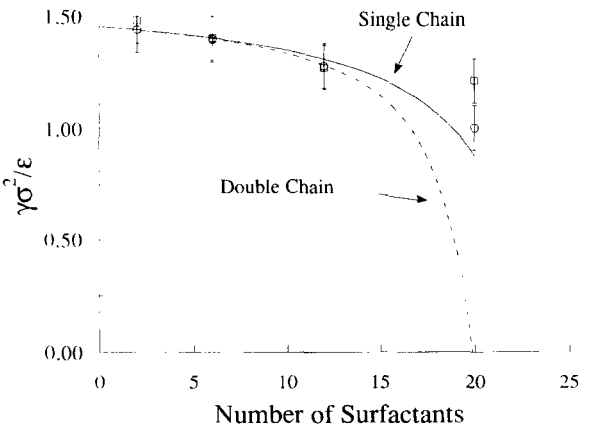

Fig. 3. The dimensionless interfacial tension ($\gamma\sigma^2/\epsilon$) vs. number of surfactants for (□) double chain, (○) single chain.

The inability of this equation of state to predict tension throughout the entire concentration range (of the dilute regime) is linked to the presence of attractive forces, which become increasingly significant as the distance between the amphiphiles decreases. Such forces act to reduce the surface pressure, and hence increase the tension. Their influence, which is not accounted for in the equation of state, controls the point and extent of departure of the actual tension from that predicted. Intuition suggests that amphiphiles having larger effective disk diameters, and thus less space between disks, should depart sooner (i.e. at smaller concentrations); this is borne out in Fig. 3 where at $N=20$ the tension of the double-chained amphiphile (4:1) lies significantly above the equation of state prediction, while that of the single-chained amphiphile (4:1) does not. Although not explicitly shown, longer (6:1) amphiphiles experience a larger deviation from their equation of state predictions than do their shorter (4:1) counterparts: not only are their disk diameters larger but they have more hydrophobic particles able to participate in attractive intermolecular interactions.

Clearly, simulation results in the dilute regime could ultimately be used to evaluate the performance of two-dimensional equations of state which take into account attractive interactions. Given the small number of tension values collected in the range where attractive interactions are important, we did not attempt to carry out such studies.

4. Conclusions

In this study, we extended the work of Smit and co-workers [13–16], examining further the influence of architecture on the tension-reducing properties of amphiphiles. In comparing single-chained to double-chained amphiphiles, we find the former to be more effective at reducing interfacial tension; this result is in accord with that of Van Os et al. [13], who investigated branched and single-chained configurations. For all amphiphiles examined, the concentration dependence of tension exhibited two nearly linear regimes. At lower

concentrations, where the tension decreases more strongly, amphiphiles reside solely at the interface, behaving essentially as insoluble monolayers. Two-dimensional equations of state can be used to model the tension behavior in this regime. At higher concentrations, amphiphiles reside both in the oil phase and at the interface, with the latter hosting a relatively constant amount. In all or some of this regime, the most stable state is probably not achieved, since under similar thermodynamic conditions Smit et al. [16] observe micelle formation in their larger-scale simulations. Nevertheless, this simple model of amphiphiles, and especially its implementation in smaller-scale computer simulations (manageable on stand-alone workstations), is a valuable tool for fundamental investigations of the behavior of amphiphiles. In future work, we plan to use this approach to study the structure and phase behavior of mixed monolayers composed of both soluble and insoluble amphiphiles.

Appendix

The harmonic potential used to create amphiphiles is characterized by a distance parameter representing the separation at zero force, and a spring constant k. Clearly this distance must be small enough, and the spring constant large enough, such that molecules can be mimicked, yet their absolute values should not influence thermodynamic properties such as the interfacial tension. We have confirmed that the strength of the spring constant does not affect tension. We performed three simulations on a system of 40 amphiphiles (made up of one hydrophilic segment and one hydrophobic segment (1:1)); shown in Table A1 are the tensions for the different values of k employed. As is readily seen, as the spring constant is varied over three orders of magnitude, only minor changes in tension are detected. As can be expected, however, the absolute value of k influences the mean separation between the connected segments (which also experience Lennard-Jones potentials): the higher the spring constant, the shorter the average distance between the amphiphile segments.

Table A1
Dimensionless interfacial tension ($\gamma\sigma^2/\epsilon$) and amphiphile separation (σ) as a function of Hookean spring constant, k (ϵ/σ^2)

Spring constant, k	Interfacial tension	Amphiphile separation
20	0.746 ± 0.10	1.214 ± 0.024
200	0.713 ± 0.09	1.060 ± 0.008
2000	0.792 ± 0.09	1.011 ± 0.004

Acknowledgments

We gratefully acknowledge the support for this work provided by the David and Lucile Packard Foundation, the National Science Foundation Presidential Young Investigator Program (grant CTS-89-57051), and a grant from the North Atlantic Treaty Organization (CRG 890971).

References

[1] J. Hautman and M.L. Klein, J. Chem. Phys., 93 (1990) 7483.
[2] J. Hautman and M.L. Klein, J. Chem. Phys., 91 (1989) 4994.
[3] J. Hautman, J.P. Bareman, W. Mar and M.L. Klein, J. Chem. Soc. Faraday Trans., 87 (1991) 2031.
[4] J.G. Harris, J. Phys. Chem., 96 (1992) 5077.
[5] S. Karaborni and S. Toxvaerd, J. Chem. Phys., 96 (1992) 5505.
[6] S. Karaboni, S. Toxvaerd, and O.H. Olsen, J. Phys. Chem., 96 (1992) 4965.
[7] G. Roberts, Langmuir–Blodgett Films, Plenum Press, New York, 1990.
[8] R.G. Larson, L.E. Scriven, and H.T. Davis, J. Chem. Phys., 83 (1985) 2411.
[9] R.G. Larson, J. Chem. Phys., 91 (1989) 2479.
[10] R.G. Larson, J. Chem. Phys., 89 (1985) 1642.
[11] M. Meyer, M. Mareschal, and M. Hayoun, J. Chem. Phys., 89 (1988) 1067.
[12] M. Mareschal, M. Meyer, and P. Turq, J. Phys. Chem., 95 (1991) 10723.
[13] N.M. van Os, L.A.M. Rupert, B. Smit, P.A.J. Hilbers, K. Esselink, M.R. Bohmer, and L.K. Koopal, Colloids Surfaces A: Physicochem. Eng. Aspects, 81 (1993) 217.
[14] B. Smit, P.A.J. Hilbers, K. Esselink, L.A.M. Rupert, N.M. van Os, and A.G. Schlijper, Nature, 348 (1990) 624.
[15] B. Smit, A.G. Schlijper, L.A.M. Rupert, and N.M. van Os, J. Phys. Chem., 94 (1990) 6933.

[16] B. Smit, P.A.J. Hilbers, K. Esselink, L.A.M. Rupert, N.M. van Os, and A.G. Schlijper, J. Phys. Chem., 95 (1991) 6361.
[17] M.M. Telo da Gama and K.E. Gubbins, Molecular Physics, 59 (1986) 227.
[18] M.P. Allen and D.J. Tildesley, Computer Simulation of Liquids, Oxford University Press, Oxford, 1987.
[19] D.K. Chattoraj and K.S. Birdi, Adsorption and the Gibbs Surface Excess, Plenum Press, New York, 1984.